Criticality of Relaxation in Dislocation Systems

Péter Dusán Ispánovity,[1,2,*] István Groma,[2] Géza Györgyi,[2] Péter Szabó,[2] and Wolfgang Hoffelner[1]

[1]*Paul Scherrer Institut, CH-5232 Villigen PSI, Switzerland*
[2]*Department of Materials Physics, Eötvös University Budapest, H-1518 Budapest POB 32, Hungary*
(Received 8 March 2011; published 16 August 2011)

Relaxation processes of dislocation systems are studied by two-dimensional dynamical simulations. In order to capture generic features, three physically different scenarios were studied and power-law decays found for various physical quantities. Our main finding is that all these are the consequence of the underlying scaling property of the dislocation velocity distribution. Scaling is found to break down at some cutoff time increasing with system size. The absence of intrinsic relaxation time indicates that criticality is ubiquitous in all states studied. These features are reminiscent of glassy systems and can be attributed to the inherent quenched disorder in the position of the slip planes.

When crystalline materials are subjected to large enough stresses they undergo plastic, irreversible deformation caused by the motion of dislocations. As is well known, these linear lattice defects interact via long-range ($1/r$-type) stress fields [1] playing a crucial role in several complex phenomena related to plasticity, such as the formation of various dislocation patterns during deformation [2] and dislocation avalanches [3]. Other systems with long-range interactions, like gravitating particles [4] or non-neutral plasmas [5], have been intensely studied and found to exhibit several unique properties, like power-law relaxation [6]. Unlike dislocations these systems are Hamiltonian; still, one would expect similar level of complexities.

Another characteristics of dislocation systems is the inherent randomness in the positions of slip planes, wherein individual dislocations glide easily. On the other hand, systems with disorder, like structural and spin glasses, have been the focus of much interest. They were found to show peculiar dynamical properties [7], such as slow relaxation, attributed to a wide spectrum of decay times. The fact that dislocation systems contain quenched disorder through the glide planes raises the analogy with spin glasses. Glassy dynamical behavior has indeed been observed in simulations [8] and experimentally [9] for dislocation systems, but the phenomenon is still lacking a systematic study.

The interplay of long-range interaction and disorder leads to complex behavior even in two-dimensional dislocation systems [10–12]. The model is a strong simplification over reality, local processes [13] were neglected, only justified by the richness of phenomena reported about in this Letter. Slow relaxation was observed in several instances, like under constant external stress, i.e., creep condition. In this case a dislocation system with single slip exhibits the well-known Andrade-type creep law [14], with the plastic strain rate $\dot{\gamma}_{pl}$ decreasing in time t as $\dot{\gamma}_{pl}(t) \sim t^{-2/3}$ until a cutoff time t_1 [15]. It was also

suggested that t_1 tends to infinity as some critical stress is approached from below, hinting at an analogy between the yielding transition and conventional phase transitions [15,16]. In addition, it was also reported that single slip random 2D dislocation systems at zero external stress relax to an equilibrium state slowly, with a relaxation time increasing with system size [17]. Such slow relaxation processes of dislocated crystals have also been observed experimentally [14,18].

In this Letter we focus on the properties of relaxation to equilibrium below the yield stress. In all arrangements studied we observe power-law decay of various quantities, a feature due to the underlying scaling of the dislocation velocity distribution. Scaling is always found to cut off at a characteristic time increasing with system size, indicating that critical behavior is not limited to a given threshold stress suggested by earlier investigations [10,15], rather, criticality is present in all states studied.

The system considered is the simplest representation of a dislocated crystal, consisting of parallel straight edge dislocations with parallel slip planes. Thus the problem is simplified to 2D. By denoting the position of the ith dislocation by $\mathbf{r}_i = (x_i, y_i)$, its Burgers vector by $\mathbf{b}_i = s_i(b, 0)$ ($s_i = \pm 1$ is the sign of the "charge"), the equation of motion of a dislocation can be written as [15]

$$\dot{x}_i = s_i \left[\sum_{j=1; j \neq i}^{N} s_j \tau_{\text{ind}}(\mathbf{r}_i - \mathbf{r}_j) + \tau_{\text{ext}}(\mathbf{r}_i) \right], \qquad \dot{y}_i = 0.$$

(1)

Here $\tau_{\text{ind}}(\mathbf{r}) = \cos(\varphi)\cos(2\varphi)r^{-1}$ is the shear stress field generated by an individual dislocation, τ_{ext} denotes the external shear stress, and N is the total number of the constituent dislocations. We note that the different physical parameters are absorbed in the length, time, and stress scales, as we measure them in $\rho^{-0.5}$, $(\rho M G b^2)^{-1}$, and $Gb\rho^{0.5}$ units, respectively, where ρ is the dislocation density, M is the dislocation mobility, and G is an elastic

constant [17]. So, in the rest of this Letter, only these dimensionless units are used.

Let us highlight the most important physical features of this conceptually simple model. First, the pair interaction is of long-range character, since it decays with $1/r$; moreover, it exhibits a complicated angular dependence with zero average. Second, the equation of motion (1) is first order, which is due to the commonly assumed overdamped nature of dislocation motion; thus the system is strongly dissipative, i.e., non-Hamiltonian. Third, the motion is constrained, since dislocations can only move parallel to the x axis. This has the important consequence that if the initial y coordinates are chosen randomly, this will represent a quenched disorder. As a result, the system never completely forgets its initial state, that is, it does not collapse into a global energy minimum, rather it gets trapped into a local minimum. Thus, the ground state of the system is frustrated leading to a glasslike dynamics [8].

In the first part of this Letter the relaxation of random dislocation systems is studied. In this scenario an equal number of positive ($s_i = 1$) and negative ($s_i = -1$) sign dislocations are placed randomly in a square-shaped area. Then, with periodic boundary conditions, the equations of motion (1) are solved numerically [17] until no considerable dislocation movement is observed (for an example simulation movie, see [19]). It is noted that due to the periodic boundary conditions, the stress field τ_{ind} is also modified; for details see [20]. The simulations were repeated with different initial configurations 13 000, 300, and 118 times for the system sizes of $N = 128$, 512, and 2048, respectively. During the relaxation of the system, the time-dependent probability distribution of the dislocation velocities $P(v, t)$ was determined numerically. (Since there is no external stress, for symmetry reasons, the velocity distributions of positive and negative dislocations are equal and symmetric.) According to Fig. 1(a) a remarkable feature of the velocity distribution is that it decays to zero as v^{-3} (for a theoretical explanation, see [21]). In addition, $P(v, t)$ tends to a Dirac-δ function (corresponding to the equilibrium state), and between an initial t_0 and a cutoff time t_1 this is described with the scaling law

$$P(v, t) = t^\alpha f(t^\alpha v). \qquad (2)$$

The exponent α was found to be $\alpha = 0.85(2)$ and the scaling function f can be well approximated by the form $f(x) \approx A/(Bx^3 + 1)$. Note that the curves plotted are always results of averaging over the statistical ensemble.

In order to investigate this scaling behavior in more detail, the mth moment $\langle |v(t)|^m \rangle$ of the absolute velocity was also determined for different m values. According to Eq. (2),

$$\langle |v(t)|^m \rangle = \int |v|^m P(v, t) dv = C_m t^{-m\alpha}, \qquad (3)$$
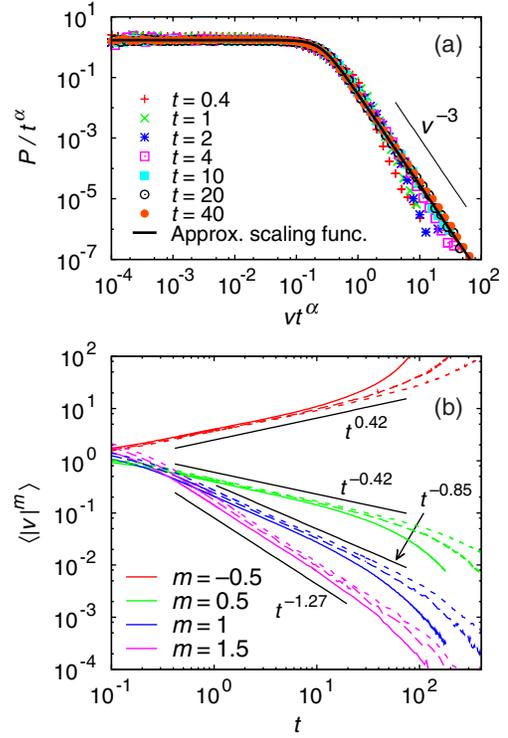

FIG. 1 (color online). Dynamics during relaxation from a random configuration. (a) The scaled velocity distributions of dislocations P given by Eq. (2) with $\alpha = 0.85$ at system size $N = 2048$, and the approximated fitted scaling function (see text). (b) The moments $\langle |v(t)|^m \rangle$ for different exponents m (m increases for the group of curves from top to bottom) and dislocation numbers N. The solid, dashed, and dotted lines correspond to $N = 128$, 512, and 2048, respectively.

where C_m is a constant. (Because of the asymptotic properties of the scaling function f, the integral is finite only for $-1 < m < 2$.) Figure 1(b) shows the measured $\langle |v(t)|^m \rangle$ curves for different m values and system sizes. The fitted exponents are in agreement with Eq. (3). (With the same simulation setup the scaling regime and the value of α have already been reported in [17].)

As seen in Fig. 1(b) the scaling region is bounded from both sides. It starts at a fixed $t_0 \approx 0.4$ and lasts till a cutoff time t_1 increasing with linear system size $L = \sqrt{N}$. This is in perfect accordance to what is usually found in systems with long-range interactions. The actual t_1 versus L relation is analyzed below.

In the second simulation scenario, an extra dislocation with fixed position is introduced to an already relaxed configuration [19]. This can be considered as the prototype of an external perturbation. (The equilibrium dislocation configuration generated by the extra dislocation, the analogue of Debye screening, was analyzed in [22,23].) Because of the extra force field, the system evolves to a new equilibrium state. As Fig. 2 shows, $P(v, t)$ again obeys the same scaling law given by Eq. (2), now with
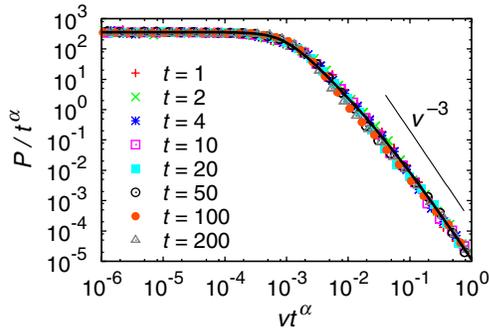
FIG. 2 (color online).   Scaling of the velocity distribution after adding an extra fixed dislocation to a relaxed system with $\alpha = 0.34$ at $N = 2048$. The corresponding scaling function (solid line) is $f(x) \approx A/(Bx^3 + Cx^2 + 1)$.

$\alpha = 0.34(4)$. Consistently, the evolution of different velocity moments obey Eq. (3), and thus confirms scaling.

In the third scenario an external constant shear stress τ_{ext} is turned on to the relaxed system [19] (creep experiment first studied by Miguel *et al.* [15]). If τ_{ext} is smaller than a certain yield stress, the induced mean plastic strain rate $\dot{\gamma}_{pl}(t)$ decreases to zero. Figure 3(a) shows the evolution of $\dot{\gamma}_{pl}$ at different external stresses τ_{ext} and system sizes N. As seen $\dot{\gamma}_{pl}$ also has a power-law regime with exponent slightly decreasing with increasing τ_{ext}. Like for the relaxation without external stress, the power decay is cut off at some time t_1, not shown in Fig. 3(a) for clarity. We again find that t_1 is increasing with system size; for more details see [19]. It is, however, practically independent from τ_{ext}, a conclusion different from what was drawn in [11,15]. Namely, there it was found that at a critical stress level $\dot{\gamma}_{pl}(t)$ becomes pure power law without a cutoff time, whereas below it a stress-dependent cutoff exists. According to our investigations for low stresses, the cutoff $t_1 \propto \sqrt{N}$ is mainly due to finite size.

We now turn to the velocity distribution of positive and negative dislocations, denoted by P^+ and P^-, respectively. For symmetry reasons the distribution always fulfills $P^+(v, t) = P^-(-v, t)$, so it is enough to investigate P^+, denoted hereafter by P. We separate it into a symmetric and an antisymmetric part as $P = P_s + P_a$ (note that in the absence of external stress $P_a = 0$, hence $P^+ = P^-$). Then in the definition of the velocity moments Eq. (3) P has to be replaced by P_s, and $\dot{\gamma}_{pl}$ is

$$\dot{\gamma}_{pl}(t) = \left\langle \sum_{i=1}^{N} s_i v_i \right\rangle = \int v P_a(v, t) dv. \quad (4)$$

Figures 3(b) and 3(c) show the scaling of P_s and P_a, respectively, for $\tau_{ext} = 0.11$ with

$$P_s(v, t) = t^\alpha f(t^\alpha v) \quad \text{and} \quad P_a(v, t) = g(t^\beta v), \quad (5)$$

at $\alpha = 0.32(2)$ and $\beta = 0.32(3)$, numerically indistinguishable in this case. Note that no power prefactor was
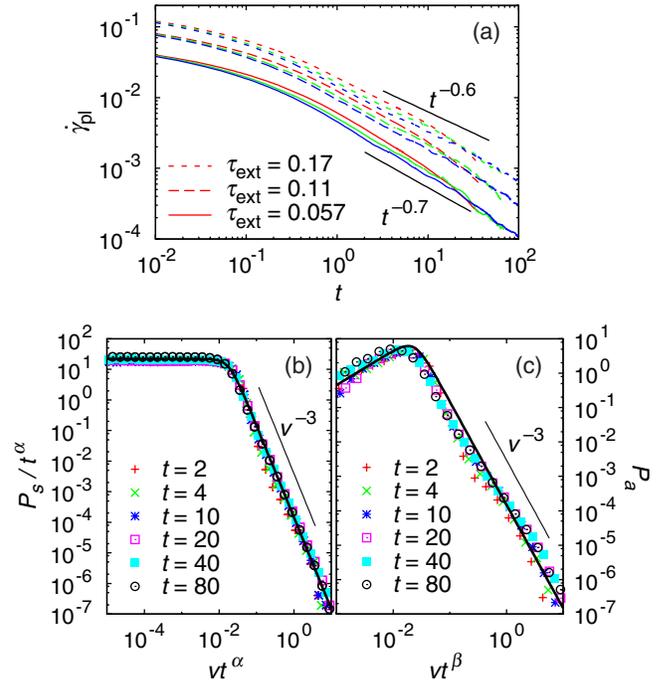

FIG. 3 (color online).   Relaxation due to a constant external shear stress τ_{ext} below the yield stress. (a) The mean plastic strain rate $\dot{\gamma}_{pl}$ versus time t curves for different τ_{ext} and system sizes N. Curves for increasing size (from top to bottom at $t = 1$; red, green, and blue) correspond to $N = 128$, 512, and 2048, respectively. The plot centers on the power-decaying regime, not resolving the cutoff times. (b) The symmetric part of the velocity distribution P_s at different times scaled with Eq. (5) with $\alpha = 0.32$ at $N = 2048$ and $\tau_{ext} = 0.11$. The approximate scaling function (solid line) is $f(x) \approx A/(Bx^3 + 1)$. (c) The antisymmetric part of the velocity distribution P_a at different times scaled with Eq. (5) with $\beta = 0.32$ at $N = 2048$ and $\tau_{ext} = 0.11$. The approximate scaling function (solid line) is $g(x) \approx C/(Dx^3 + x^{-1})$.

found in the scaling form of P_a above. From Eqs. (4) and (5) $\dot{\gamma}_{pl}(t) = Ct^{-2\beta}$, with an appropriate C constant. This is in complete agreement with the time evolution of $\dot{\gamma}_{pl}$ plotted in Fig. 3(a). For different τ_{ext} values, the same scaling is found with slightly different exponents. We mention that the plastic strain $\gamma_{pl}(t)$ has the exponent $1 - 2\beta$, this varies in the range 0.3–0.4, and is in accordance with the well-known power $1/3$ of the Andrade creep [14,15].

To summarize the above findings, the scaling formulas Eq. (5) seem to be generally valid. The exponents vary, however, a feature we attribute to the difference in the initial conditions and external stress field, the only properties distinguishing the scenarios we considered. Thus, the exponent is not a universal, inherent characteristic of the dislocation system determined only by the interactions and dimensionality.

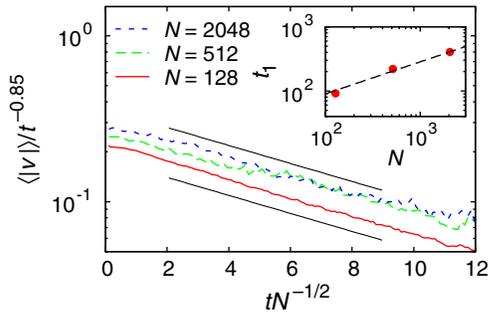The last issue to be elucidated is the system size dependence of the cutoff time t_1. In order to determine t_1,

FIG. 4 (color online). Rescaled mean absolute velocity $t^\alpha\langle|v(t)|\rangle$ as a function of scaled time $t/\sqrt{N}$ at different system sizes. Straight line on the semilog plot shows the exponential component, defining a relaxation time t_1 for each N. Inset shows the obtained t_1 values and the $t_1 \sim \sqrt{N}$ fit.

$t^\alpha\langle|v(t)|\rangle$ is plotted with a semilogarithmic scale in Fig. 4 for the first simulation scenario. As seen, the curves obtained can be well fitted by straight lines, so the time evolution of $\langle|v|\rangle$ can be described with the form $\langle|v(t)|\rangle = Ct^{-\alpha}\exp(-t/t_1)$. Thus the cutoff time t_1 is a simple relaxation time.

In addition, in Fig. 4 the time is rescaled with $L = \sqrt{N}$ and with this the curves corresponding to different system sizes are parallel, indicating that t_1 is proportional to the system size L. Similar behavior is found for the different order velocity moments introduced above. These results indicate that the relaxation of $\langle|v(t)|\rangle$ can be described with the rate equation

$$\frac{d\langle|v(t)|\rangle}{dt} = -\left(\frac{\alpha}{t} + \frac{1}{t_1}\right)\langle|v(t)|\rangle, \qquad (6)$$

where $t_1 \propto L$. This can be interpreted as follows: at large enough time ($t \gg t_1$) during the relaxation of a dislocation system with finite size it always gets close to its energy minimum and enters into an exponential relaxation regime. With increasing system size, however, the energy landscape becomes more and more complex, resulting in a longer time to reach the exponential relaxation regime. This is in agreement with the recent results of Laurson *et al.* [10], who found that the dynamics slows down dramatically as the yield stress is approached from above. We would also like to highlight that although the time exponent α varies with conditions of the relaxation, the size dependence of the cutoff time t_1 is in all scenarios studied in this Letter close to linear [19].

In summary, power-law relaxation of dislocation systems was observed in different scenarios. This effect may be attributed to the quenched random positions of the slip axes and the complex nature of the interactions. Remarkably, the scaling of the time-dependent velocity distribution goes with different exponents depending on the physical setup. Scaling is cut off due to the finite size, so the system does not possess any inherent time scale. The dislocation system is, therefore, found to behave like a critical one in all cases considered, strongly resembling glassy systems.

*ispanovity@metal.elte.hu; http://dislocation.elte.hu
[1] J. P. Hirth and J. Lothe, *Theory of Dislocations* (John Wiley & Sons, New York, 1982), 2nd ed.
[2] M. Zaiser and A. Seeger, *Dislocations in Solids* (North-Holland, Amsterdam, 2002), Vol. 11, pp. 1–100.
[3] F. F. Csikor, C. Motz, D. Weygand, M. Zaiser, and S. Zapperi, Science **318**, 251 (2007).
[4] T. Padmanabhan, Phys. Rep. **188**, 285 (1990).
[5] D. R. Nicholson, *Introduction to Plasma Theory* (Wiley, New York, 1983).
[6] A. Campa, T. Dauxois, and S. Ruffo, Phys. Rep. **480**, 57 (2009).
[7] V. Ilyin, I. Procaccia, I. Regev, and N. Schupper, Phys. Rev. E **77**, 061509 (2008).
[8] B. Bakó, I. Groma, G. Györgyi, and G. T. Zimányi, Phys. Rev. Lett. **98**, 075701 (2007).
[9] S. J. Gerbode, U. Agarwal, D. C. Ong, C. M. Liddell, F. Escobedo, and I. Cohen, Phys. Rev. Lett. **105**, 078301 (2010).
[10] L. Laurson, M.-Carmen Miguel, and M. J. Alava, Phys. Rev. Lett. **105**, 015501 (2010).
[11] J. Rosti, J. Koivisto, L. Laurson, and M. J. Alava, Phys. Rev. Lett. **105**, 100601 (2010).
[12] G. Tsekenis, N. Goldenfeld, and K. A. Dahmen, Phys. Rev. Lett. **106**, 105501 (2011).
[13] D. Gómez-García, B. Devincre, and L. P. Kubin, Phys. Rev. Lett. **96**, 125503 (2006).
[14] F. Nabarro, Acta Mater. **54**, 263 (2006).
[15] M.-Carmen Miguel, A. Vespignani, M. Zaiser, and S. Zapperi, Phys. Rev. Lett. **89**, 165501 (2002).
[16] M. Zaiser, Adv. Phys. **55**, 185 (2006).
[17] F. F. Csikor, M. Zaiser, P. D. Ispánovity, and I. Groma, J. Stat. Mech. (2009) P03036.
[18] F. Louchet and P. Duval, Int. J. Mat. Res. **100**, 1433 (2009).
[19] See Supplemental Material at http://link.aps.org/supplemental/10.1103/PhysRevLett.107.085506 for movies on single relaxation runs and illustration of cutoff times.
[20] B. Bakó, I. Groma, G. Györgyi, and G. Zimányi, Comput. Mater. Sci. **38**, 22 (2006).
[21] P. D. Ispánovity, I. Groma, G. Györgyi, F. F. Csikor, and D. Weygand, Phys. Rev. Lett. **105**, 085503 (2010).
[22] I. Groma, G. Györgyi, and B. Kocsis, Phys. Rev. Lett. **96**, 165503 (2006).
[23] P. D. Ispánovity, I. Groma, and G. Györgyi, Phys. Rev. B **78**, 024119 (2008).